PLASMA PROCESS ANALYSIS OF ICP-PECVD OF ALOX LAYERS FOR C-SI SURFACE PASSIVATION

M. Hofmann[1], M. Jäcklein[1], P. Saint-Cast[1], D. Wagenmann[1], B. Cord[2], T. Dippell[2], M. Dörr[2], T. Schütte[3], M. Siemers[4]
[1]Fraunhofer Institute for Solar Energy Systems ISE, Heidenhofstrasse 2, 79110 Freiburg, Germany
[2]SINGULUS Technologies AG, Hanauer Landstrasse 103, 63796 Kahl am Main, Germany
[3]PLASUS GmbH, Lechstrasse 9, 86415 Mering, Germany
[4]Fraunhofer Institute for Surface Engineering and Thin Films IST, Bienroder Weg 54E, 38108 Braunschweig, Germany

ABSTRACT: The detailed analysis of the ICP-PECVD plasma process using spectroscopic plasma monitoring and the ex-situ analysis of the manufactured layers and interfaces to the c-Si substrates provide insight into the interdependency of passivation mechanisms and process conditions. Plasma process simulations based on the particle-in-cell Monte Carlo method additionally allowed getting insight into electron density and electron energy distributions. The combination of these measures lead to highly passivating very thin AlO_x layers of thicknesses below 5 nm allowing to lower the cost of ICP-PECVD AlO_x deposition.
Keywords: passivation, PECVD, AlO_x, plasma monitoring

1 INTRODUCTION

In 2015, more and more passivated emitter and rear cell (PERC) –type [1] solar cell production facilities were installed on industrial level. This trend is expected to go on and lead to a significant market share of PERC-type cells in the near future. One very attractive route for the implementation of the industrial rear passivation technology is the application of plasma-enhanced chemical vapor deposition (PECVD) of aluminum oxide (AlO_x) [3] [5]. Its attraction is driven by the industrially proven PECVD technology already applied for decades for the front side anti-reflection coating (ARC) using silicon nitride (SiN_x) layers. PECVD will stay in use for the ARC application; therefore it is very logic to use the same technology for the AlO_x deposition as well. On the other hand, despite a successful proof in literature for a very high surface passivation quality possible by PECVD AlO_x the competition with atomic layer deposition (ALD) of AlO_x layers is still ongoing.
PERC-type cells which are becoming increasingly important in industrial production but also almost all other kinds of advanced crystalline silicon solar cell concepts (PERL, PERT, IBC, …) are depending on an effective surface passivation technology for reaching highest energy conversion efficiencies. Built-in negative charges in AlO_x on c-Si are creating a beneficial band bending at the p-type c-Si PERC rear surface.
This paper will focus on the analysis of PECVD-AlO_x layers deposited by an inductively coupled plasma (ICP) using in-situ and ex-situ experimental and simulative methods in order to increase the understanding of the plasma process and to enhance passivation quality, especially for very thin layers below 5 nm. The reduction of AlO_x layer thickness will allow to further reduce the process cost for AlO_x passivation layers, mainly due to an increase in wafer throughput per hour and a decreasing use of consumables per wafer.

2 EXPERIMENTAL

ICP-PECVD allows very effective gas dissociation [2] due to the very high plasma density and therefore high ionization of the gas species. In this work, a SINGULUS Singular ICP-PECVD tool was applied for the fabrication of thin AlO_x layers. Sketches of the tool can be found in Figure 1 and Figure 2. Figure 2 elucidates the way the wafers are taken through the deposition tool. A carrier with four 156x156 mm^2 wafers enters the vacuum through the load lock and then is moved clockwise to the IR station and onwards to the AlO_x and the three SiN_y stations. Here, the ICP-sources operating at 13.56 MHz are mounted and are process gas-separated by individual vacuum locks.
The deposition experiments and carrier lifetime investigations were carried out using float-zone (FZ) monocrystalline silicon wafers (p-type, boron doped) with a resistivity of 1…1.5 Ω cm and a thickness of about 250…300 µm.

Figure 1: SINGULUS Singular PECVD tool applied in the investigations here [10].

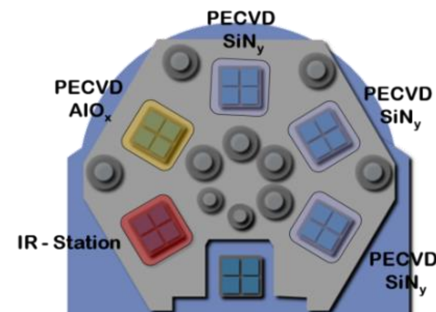

Figure 2: Deposition station top view schematic of the Singular PECVD tool showing the load lock at the bottom of the image, IR station for wafer heating and the deposition chambers for AlO_x and SiN_y. Since the SiN_y layers are typically prepared much thicker than the AlO_x layer, three SiN_y stations are used sequentially. For all process stations, the same process time is available due to the synchronized clockwise movement of the 4 wafers from one process station to the other. See also [10].

Plasma analysis applying spectroscopic plasma monitoring (SPM) technique based on optical emission spectroscopy (OES) provides deep time-resolved insights into the dynamics of the plasma species. Therefore, it can be recognized what kinds of species are present and how to control their ratios. In the investigations presented here, a PLASUS EMICON 3MC system was applied. The analysis of the emitted spectra was partly performed using the actinometry method where the spectra are normalized to a non-reactive gas which was in our case the emission from the argon gas being kept at constant partial pressure throughout the experiments.

The combination of this in-situ characterization method with ex-situ analysis of the created layers is of benefit to achieve a correlation of parameters and an optimization. Contactless capacitance-voltage (COCOS, applying a Semilab SDI CFORS tool), spectroscopic ellipsometry (SE, applying a J. A. Woollam M-2000 tool) and carrier lifetime measurements (QSSPC, WCT-120 tool by Sinton Instruments) were performed. Detailed characteristics of the plasma technology were elucidated by particle-in-cell Monte Carlo (PIC-MC) simulations of the ICP-PECVD process chamber [4] providing local electron temperature and electron density distributions in the PECVD reactor that can facilitate an efficient deposition process.

Since PERC-type and other solar cell types applying passivated surfaces are becoming increasingly important not only in academia but also industrially, a thorough understanding of the AlO_x deposition process is of high relevance and allows for stable and highly efficient processes.

One goal of the investigations presented here is the reduction of the AlO_x layer thickness from 20-30 nm to 5 nm or even less still allowing the same excellent surface passivation properties.

3 RESULTS

3.1 Plasma simulations

For the simulation of the AlO_x deposition plasma process, the setup of the process chamber was used as sketched in Figure 3 which is in accordance with the actual reactor geometry.

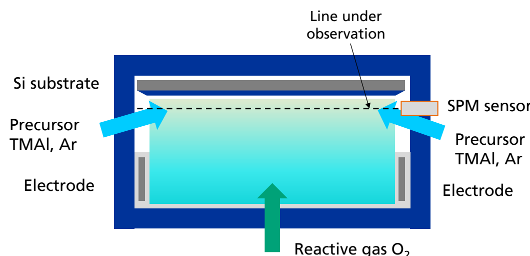

Figure 3: Schematic drawing of the setup of the AlO_x deposition chamber. The deposition takes place via the plasma which is located below the substrates. The reactive gas (oxygen-containing in the case of AlO_x deposition) is passing the inductively coupled plasma (ICP) and gets dissociated. The precursor gas (trimethylaluminum TMAl) is entering the deposition chamber near the substrates. A spectroscopic plasma monitoring (SPM) sensor is installed to observe the plasma close to the substrate.

PIC-MC plasma simulations are one fundamental tool to understand the physics occurring in the PECVD process.

Figures 4 and 5 show simulated electron density and electron energy distributions for a 2D cross section through the reaction chamber. The simulations were performed with argon as working gas. Argon is often used for benchmarking and with argon experimental plasma measurements are easily done to compare against the simulations. Additionally, the applied power was about 1/100 of the reality due to limitations in the simulation. However, it is expected that the simulation results still allow qualitatively correct interpretations.

In the conducted simulations, a variation of the process pressure was applied with p=2 Pa in Figure 4 and p=10 Pa in Figure 5. Increasing the gas pressure leads to higher plasma density and lower electron energy. This higher plasma density causes more shielding of the inner plasma volume resulting in a stronger plasma confinement in close vicinity of the electrode. Electron densities up to 3×10^{15} m^{-3} or 9×10^{15} m^{-3} and low maximum electron energies of 3.4 eV or 2.5 eV for process pressures of p=2 Pa or p=10 Pa, respectively, were results of the simulation. Low electron energies are typical for an ICP –plasma generating low voltages and thus avoiding high energy ions which could damage the cell surface. The electron densities are relatively low which can be attributed to the low RF power (13.56 MHz) applied in the simulation compared to the real power used in the experimental setup. In the electron density distribution, one can find the "secondary coil" shape of the ICP setup.

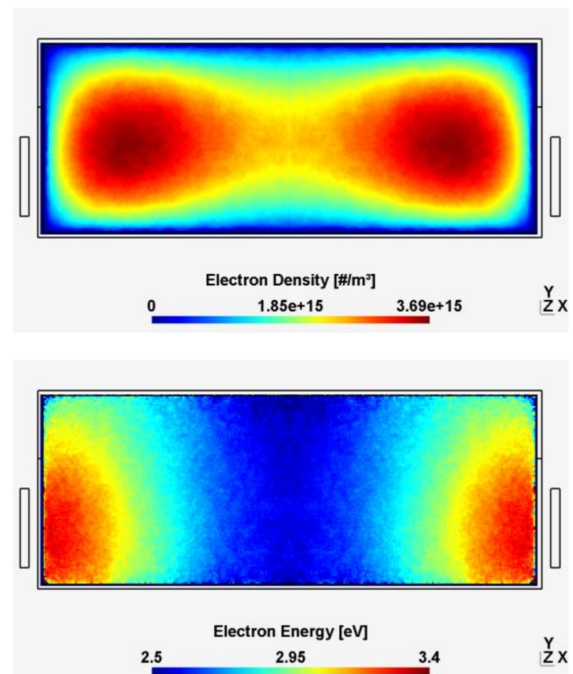

Figure 4: To investigate general plasma behaviour, intense simulations were carried out using the particle-in-cell Monte Carlo (PIC-MC) method.

The upper and lower parts show the two dimensional distributions of electron density and electron energy, respectively, in the reactor vessel (horizontal width about 500 mm) for a gas (Ar) pressure of p=2 Pa.

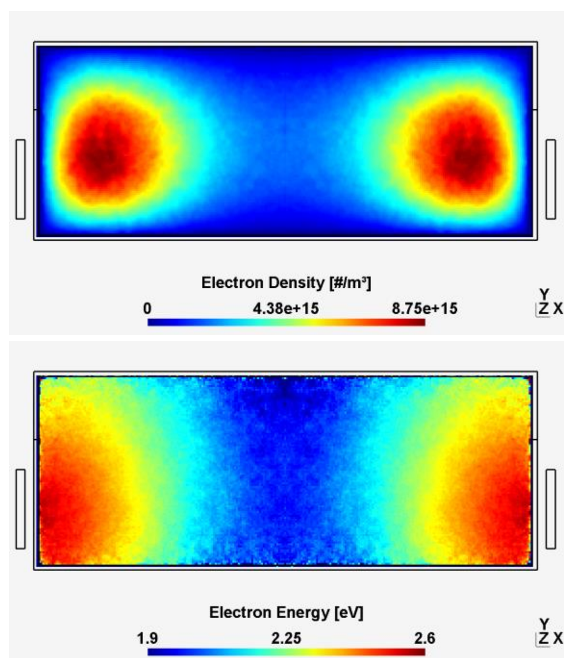

Figure 5: PIC-MC simulation results of electron density (top) and electron energy (bottom) for a process pressure of p=10 Pa. Please compare to Figure 4.

3.2 In-situ plasma monitoring investigation

Spectroscopic plasma monitoring (SPM) based on optical emission spectroscopy was used to observe the plasma created for the deposition of AlO_x layers. A gas mixture of trimethylaluminum (TMAl, $Al(CH_3)_3$), oxygen (O_2), and argon (Ar) was applied. In the photon spectrum, a lot of optical emission lines could be detected and assigned to various atoms or molecules in the plasma with the main contributions from species like Ar, H, O, Al and AlO. Since Ar is inert and an Ar emission line is separated from all others, one can use it as base for an actinometric analysis of the data. Actinometry was presented by Coburn and Chen. More information can be found in [6]. Shortly, the Ar signal can be used to normalize the other signals and to allow an easier cross-interpretation over different parameter sets including start-up and shut-down characteristics.

One example of an investigated process can be found in Figure 6 and Figure 7. Figure 6 shows a typical spectrum of the process with the spectral lines of the observed species. In Figure 7 the temporal behavior of the species over process time are presented where the top graph shows the data as acquired and the bottom graph's data underwent an actinometric calculation.

In the case presented here with each deposition cycle taking 7.5 s we find that in the first 1.8 s after switching on the plasma, start-up conditions occur for the formation of the different gas species after the plasma ignition. A peak of H is most prominent. H must be coming from cracked TMAl molecules. Since H is beneficial for interface passivation, enough visible H in the spectra can be interpreted as a first positive sign for the surface passivation properties of the layer. At the same time, the amount of detected O species is relatively slowly increasing to a saturation value. One might wonder why the oxygen signal is so small in the start-up phase. We see that during start-up AlO species are providing an increased emission behavior showing that the formation of these species is one drain for oxygen. Thus, a very effective decomposition of TMAl in the beginning of the plasma process and/or the presence of a large amount of TMAl seems to occur which provides bonding partners for oxygen in form of AlO, OH and presumably other species such as CO_x as well. This is leading to stable process conditions after about 1.8 s.

The very steep curves in the lower graph at t=0 s are due to actinometric calculations and should not be over-interpreted.

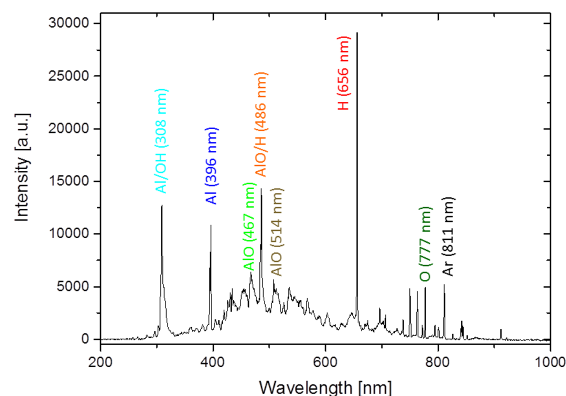

Figure 6: An example of a plasma monitoring spectrum.

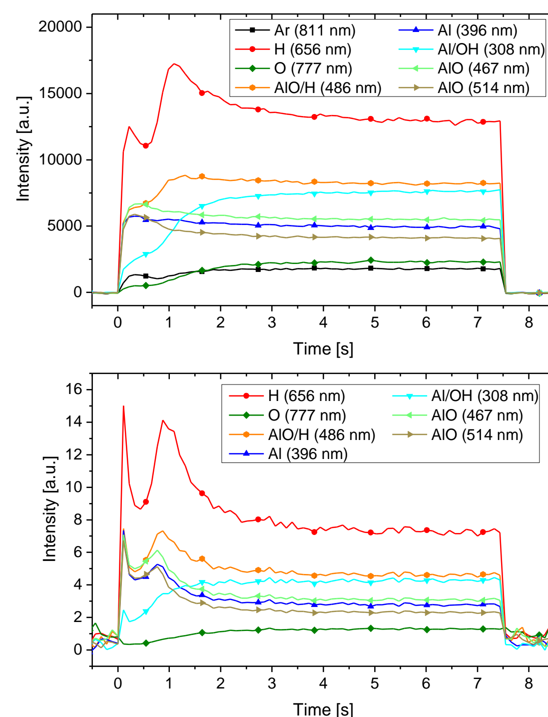

Figure 7: An example of gas dynamics within one deposition cycle is shown as acquired with spectroscopic plasma monitoring (SPM) technique. The intensity on the y-axis equals the relative counts of photons at the mentioned spectral lines. The different species can be identified and separated. Aluminium and/or oxygen-containing species create the AlO_x layer. Hydrogen plays an additional crucial role in the creation of highly passivating layers due to its ability to lower surface defect density. Since Argon is inert, one can use it as reference gas for further analysis based on actinometry.

Top: SPM data as acquired.

Bottom: SPM data after actinometry based on Ar.

3.3 Ex-situ investigation of layer and interface properties

PECVD process parameter variations were carried out with simultaneous plasma monitoring and deposition of passivating AlO_x layers on wafer samples. One of these investigations was focussing on an O_2 flux variation. Here, the O_2 flux was changed from 20% to 100% (relative units) while keeping all other process parameters constant. The process pressure was increased slightly due to the higher total gas flux. Figure 8 shows an overview of the lifetime results. A strong increase of lifetime was found for relatively low oxygen fluxes. In Figure 9, plasma monitoring spectra of the O line (right) and the H line (left) in dependency of the O_2 gas flux at constant flux of the aluminum precursor in the PECVD process, after actinometric data analysis, are displayed. The oxygen signal (λ=777 nm) is increased as expected for the process with higher O_2 gas flux. However, the H signal is decreased with increasing O_2 flux.
We assume that the decreased H signal correlates to the observed lifetime reduction, probably due to a reduced level of H incorporation in the passivating AlO_x layer. Also the AlO signal is increased with increasing O_2 flux (not displayed as graph here) indicating a more prominent presence of AlO compounds already in the gas phase. The influence of these compounds on the AlO_x layer structure, the interface defect density (D_{it}) and the negative charge density (Q_{tot}) is subject to further investigation.

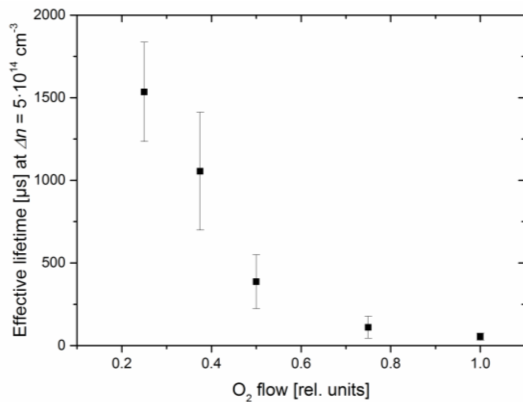

Figure 8: Effective carrier lifetime as a function of the O_2 gas flux (given in relative units).

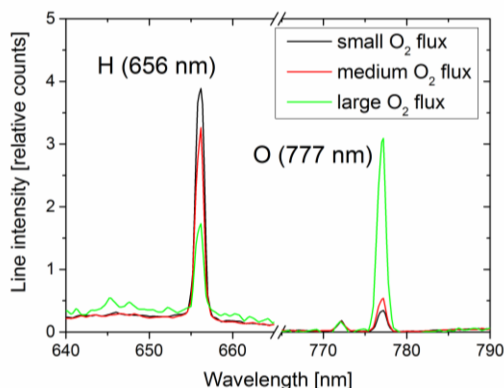

Figure 9: Plasma monitoring spectra of the O line (right) and the H line (left) in dependency of the O_2 gas flux at constant flux of the aluminum precursor in the PECVD process, after actinometric data analysis.

Just like the variation of the O_2 flux, also other process parameters can play a crucial role on the passivation results. However, it is possible to find robust high-quality processing setups.
Contactless capacitance-voltage (COCOS) measurements were performed to investigate the physical mechanisms behind the passivation results. Figure 10 provides an overview. The exact details of the process conditions are not given in this paper. However, one can see the range of results. In Figure 10, the lifetime results are additionally represented in the colors and heights of the data points. The surface preparation process variation is labelled with a small letter, the deposition process variation with a capital letter. Deposition process H allows excellent surface passivation almost independent of the preconditioning of the wafer surface (within the applied frame here). The passivation quality of layers deposited by process A is significantly depending on the surface preparation.
Thus, one can find combinations of surface preconditioning and passivation that allow high quality.

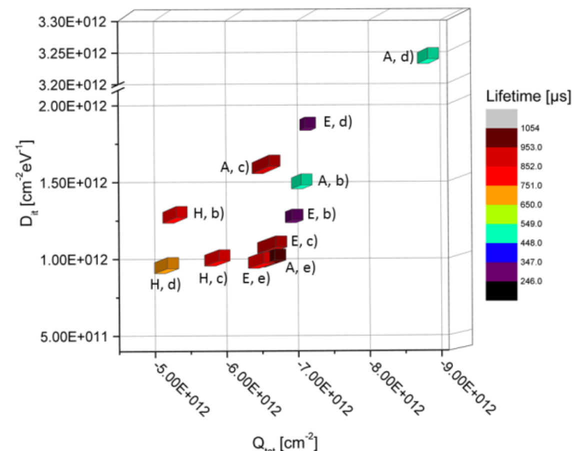

Figure 10: Contactless capacitance-voltage (COCOS, corona oxide characterization of semiconductor) measurements of differently prepared surfaces applied to different deposition parameters. Optimum processing leads to the lowest D_{it} and the highest negative Q_{tot} values. For example: Following the results for samples with 1 x 10^{12} cm^{-2} eV^{-1} one can find increasing lifetimes with increasing negative charge density.

As a result of the investigations, the AlO_x layer thickness could be lowered to ranges below 5 nm with very good passivation results as shown in Figure 11 which were comparable to thick ICP-PECVD AlO_x layers of about 18 nm thickness and to a variety of ALD passivation results from the literature [7-8] [11]. MW-PECVD AlO_x layers were reported to show significant lifetime decrease starting at ~10 nm [9].

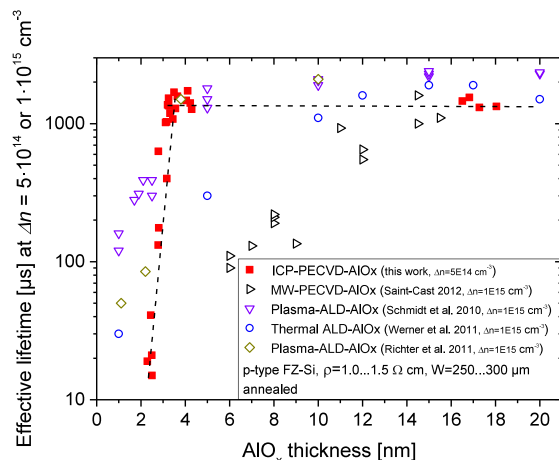

Figure 11: Carrier lifetimes of c-Si wafers with AlO_x layers of thicknesses in the range up to 20 nm on both sides after annealing (FZ-Si substrates 1.0…1.5 Ω cm, p-type, 250…300 µm). A slight variation of the O_2 flux provided the data behind the red ICP-PECVD symbols shown. It seems evident that the deposition process is quite robust in this parameter range. With changing O_2 flux, still excellent passivation properties were possible. Lifetimes of about 1.7 ms reflect a surface recombination velocity of about 5 cm/s. For comparison, also ALD-AlO_x and PECVD-AlO_x passivation layers on comparable substrate types from literature [7-9] [11] are shown.

4 CONCLUSION

Using the knowledge from the manifold analyses it was possible to deposit ICP-PECVD AlO_x layers with a thickness of only 3-4 nm that provide excellent surface passivation with a surface recombination velocity of ~5 cm/s which is comparable to the passivation quality of thicker (18 nm) ICP-PECVD-AlO_x layers and of thin ALD-AlO_x layers and would allow excellent solar cell efficiencies. A relatively robust process could be found that is capable to compensate for potential variations in gas flow during deposition. In-situ spectroscopic plasma monitoring and ex-situ analyses revealed the dynamic behavior of plasma species which can be used to understand and optimize the PECVD process. Contactless CV measurements confirmed that low interface trap densities (D_{it}) and high densities of negative charges (Q_{tot}) in the AlO_x layer are possible and lead to an excellent surface passivation. Simulations of the plasma revealed that the electron density and temperature distribution strongly depend on the process pressure and that the shape of the distribution function is based on the reactor and electrode geometry.

ACKNOWLEDGEMENT

This work was partly funded by the German Federal Ministry for the Environment, Nature Conservation and Nuclear Safety (Contract Number 0325754D).

6 REFERENCES

[1] Blakers, A. W.; Wang, A.; Milne, A. M.; Zhao, J.; Green, M. A. (1989): 22.8% efficient silicon solar cell. Applied Physics Letters 55 (13), pp. 1363–1365. DOI: 10.1063/1.101596.

[2] Lieberman, M. A.; Lichtenberg, A. J. (1994): Principles of plasma discharges and materials processing: John Wiley & Sons.

[3] Saint-Cast, P.; Kania, D.; Hofmann, M.; Benick, J.; Rentsch, J.; Preu, R. (2009): Very low surface recombination velocity on p-type c-Si by high-rate plasma-deposited aluminum oxide. Applied Physics Letters 95 (15), p. 151502. DOI: 10.1063/1.3250157.

[4] Pflug, A.; Siemers, M.; Melzig, T.; Schäfer, L.; Bräuer, G. (2014): Simulation of linear Magnetron Discharges in 2D and 3D, Surface and Coatings Technology 260 (2014) 411-416.

[5] Veith, B.; Dullweber, T.; Siebert, M.; Kranz, C.; Werner, F.; Harder, N.-P.; Schmidt, J.; Roos, B.F.P.; Dippell, T.; Brendel, R. (2012): Comparison of ICP-AlOx and ALD-Al2O3 layers for the rear surface passivation of c-Si Solar cells. In: Energy Procedia 27 (2012) 379-384.

[6] Coburn, J.W.; Chen, M., Optical emission spectroscopy of reactive plasmas: A method for correlating emission intensities to reactive particle density, Journal of Applied Physics 51 (6) (1980) 3134–3136.

[7] Schmidt, J.; Veith, B.; Werner, F.; Zielke, D.; Brendel, R. (2010): Silicon surface passivation by ultrathin Al2O3 films and Al2O3/SiNx stacks, Proceedings of the 35th IEEE Photovoltaic Specialist Conference, pp. 885-890.

[8] Werner, F.; Veith, B.; Zielke, D.; Kühnemund, L.; Tegenkamp, C.; Seibt, M.; Brendel, R.; Schmidt, J.: Electronic and chemical properties of the c-Si/Al2O3 interface, Journal of Applied Physics 109, 113701 (2011)

[9] Saint-Cast, P: Passivation of Si Surfaces By PECVD Aluminum Oxide, PhD Thesis, University of Konstanz, 2012

[10] Roos, B.F.P.; Dippell, T.; Hohn, O.; Wohlfart, P.; Beier, B.; Veit, B.; Siebert, M.; Dullweber, T.: ICP-PECVD Production Tool For Industrial AlOx and Si-based Passivation Layers, 27th EUPVSEC, pp. 1684-1687, 2012

[11] Richter, A.; Benick, J.; Hermle, M.; Glunz, Stefan W.: Excellent silicon surface passivation with 5 Å thin ALD Al2O3 layers: Influence of different thermal post-deposition treatments, Phys. Status Solidi RRL 5, No. 5–6, 202– 204 (2011)